

Short-Range Correlations and the Nuclear EMC Effect in Deuterium and Helium-3

E.P. Segarra,¹ J.R. Pybus,¹ F. Hauenstein,^{1,2} D.W. Higinbotham,³ G.A. Miller,⁴
E. Piassetzky,⁵ A. Schmidt,⁶ M. Strikman,⁷ L.B. Weinstein,² and O. Hen^{1,*}

¹*Massachusetts Institute of Technology, Cambridge, Massachusetts 02139, USA*

²*Old Dominion University, Norfolk, Virginia 23529*

³*Thomas Jefferson National Accelerator Facility, Newport News, Virginia 23606*

⁴*Department of Physics, University of Washington, Seattle, WA 98195-1560, USA*

⁵*School of Physics and Astronomy, Tel Aviv University, Tel Aviv 69978, Israel*

⁶*George Washington University, Washington, DC 20052, USA*

⁷*Pennsylvania State University, University Park, PA, 16802*

(Dated: July 14, 2020)

The EMC effect in deuterium and helium-3 is studied using a convolution formalism that allows isolating the impact of high-momentum nucleons in short-ranged correlated (SRC) pairs. We assume that the modification of the structure function of bound nucleons is given by a universal (i.e. nucleus independent) function of their virtuality, and find that the effect of such modifications is dominated by nucleons in SRC pairs. This SRC-dominance of nucleon modifications is observed despite the fact that the bulk of the nuclear inelastic scattering cross-section comes from interacting with low-momentum nucleons. These findings are found to be robust to model details including nucleon modification function parametrization, free nucleon structure function and treatment of nucleon motion effects. While existing data cannot discriminate between such model details, we present predictions for measured, but not yet published, tritium EMC effect and tagged nucleon structure functions in deuterium that are sensitive to the neutron structure functions and bound nucleon modification functions.

INTRODUCTION

Determining the underlying cause of the modification of the partonic structure of nucleons bound in atomic nuclei, known as the EMC effect [1–7], is an outstanding question in nuclear physics. Decades after its discovery, there is still no universally accepted explanation for the origin of the EMC effect [8–10], despite a large number of high-precision measurements in a wide variety of atomic nuclei.

Modern models of the EMC effect account for both ‘conventional’ nuclear physics effects such as Fermi-motion and binding, as well as for the more ‘exotic’ effects of nucleon modification [9, 10]. The conventional nuclear physics effects are well understood and cannot reproduce experimental data alone, especially when including Drell-Yan data [10, 11]. While required to reproduce experimental data, nucleon modification models are far less constrained and their microscopic origin is debated [10].

An observed correlation between the magnitude of the EMC effect and the relative amount of short-range correlated (SRC) nucleon pairs in different nuclei [7, 12–14] suggests that the EMC effect is driven by the modification of nucleons in SRC pairs. SRCs are pairs of strongly interacting nucleons at short distances. Nucleons in SRC pairs have large spatial overlap between their quark distributions and are highly offshell ($E^2 \neq |\mathbf{p}|^2 + m^2$), which makes them prime candidates for structure modification.

Most recently, it has been demonstrated [7, 15] that the EMC effect in nuclei from helium-3 (${}^3\text{He}$) to lead can be explained by a single effective universal modification

function (UMF) of nucleons in SRC pairs. The UMF was constructed to be as model-independent as possible. It is insensitive to the largely-unknown free-neutron structure function, F_2^n , and accounts for both conventional nuclear effects, such as the scheme dependence of the deuteron wave-function, and nucleon motion effects, as well as more exotic nucleon modification effects.

Here we study the EMC effect using a convolution formalism that allows us to separate the mean field and short range correlation contributions of nucleon modification effects to the total UMF. We consider only light nuclei (the deuteron and ${}^3\text{He}$), for which exact nuclear wave functions are available, and nucleon modification effects can be isolated. The sensitivity of the convolution formalism to parametrization of the nucleon modification function, F_2^n , and the treatment of nucleon motion effects are studied.

We find that, as expected, the bulk of the structure-function comes from interactions with low-momentum nucleons. However, nucleon modification effects, which are required for a complete reproduction of the measured data, are dominated by nucleons in SRC pairs. We also find that existing data cannot discriminate between different F_2^n models or different parameterizations of bound nucleon modification functions. We predict new observables that can constrain these model inputs, including the tritium EMC effect, sensitive to F_2^n , and deuterium tagged nucleon structure functions, sensitive to bound nucleon modification functions. These predictions will soon be tested by data from the MARATHON [16], BAND [17], and LAD [18] Collaborations.

FORMALISM

F_2^A Convolution Approximation

In order to study the EMC effect in a framework that allows us to understand its dependence on nucleon momentum and offshellness, we calculate the nuclear structure function, $F_2^A(x_B)$, using the nuclear convolution model for lepton-nucleus DIS [8, 19–22]:

$$\begin{aligned}
 F_2^A(x_B) &= \\
 &\frac{1}{A} \int_{x_B}^A \frac{d\alpha}{\alpha} \int_{-\infty}^0 dv \left[Z\tilde{\rho}_p^A(\alpha, v) F_2^p(\tilde{x}) + N\tilde{\rho}_n^A(\alpha, v) F_2^n(\tilde{x}) \right] \\
 &\quad \times \left(1 + v f^{off}(\tilde{x}) \right) \\
 &= \frac{1}{A} \int_{x_B}^A \frac{d\alpha}{\alpha} \int_{-\infty}^0 dv F_2^p(\tilde{x}) \left[Z\tilde{\rho}_p^A(\alpha, v) + N\tilde{\rho}_n^A(\alpha, v) \frac{F_2^n(\tilde{x})}{F_2^p(\tilde{x})} \right] \\
 &\quad \times \left(1 + v f^{off}(\tilde{x}) \right), \tag{1}
 \end{aligned}$$

where $x_B = Q^2/(2m_N\nu)$, Q^2 is the four momentum transfer squared, m_N is the nucleon mass and ν is the energy transfer (Fig. 1). $\tilde{x} = \frac{Q^2}{2p \cdot q}$ where q is the four-momentum of the virtual photon and p is the initial four-momentum of the struck off-shell nucleon. \tilde{x} reduces to $\frac{x_B}{\alpha} \frac{m_N A}{m_A}$ in the Bjorken limit with lightcone momentum fraction $\alpha = A(E + p_z)/m_A$ (see online supplementary materials for finite energy corrections to Eq. 1 at low Q^2). Here z is opposite to the direction of the virtual photon, and $v = (E^2 - |\mathbf{p}|^2 - m_N^2)/m_N^2$ is the bound nucleon fractional virtuality. $\tilde{\rho}_N^A(\alpha, v)$ are the nucleon ($N = p$ or n) lightcone momentum and virtuality distributions in nucleus A , defined below. $F_2^p(\tilde{x})$ and $F_2^n(\tilde{x})$ are the free proton and neutron structure functions. For brevity we omit their explicit Q^2 dependences but note that F_2^p , F_2^n , and F_2^A are always evaluated at the same Q^2 value. $f^{off}(\tilde{x})$ is a universal offshell nucleon modification function, assumed here to be the same for neutrons and protons and for all nuclei. In Eq. 1, we take the offshell effect to be linear in v (i.e. $1 + v f^{off}(\tilde{x})$) as a first-order Taylor expansion in virtuality; see Ref. [23] for additional discussion.

Lightcone densities

In our convolution, traditional nuclear contributions to the EMC effect such as nucleon motion and binding are treated within the one-body lightcone momentum and virtuality distribution, $\tilde{\rho}_N^A(\alpha, v)$. It describes the joint probability to find a nucleon (n or p) in a nucleus A with lightcone momentum fraction α and fractional virtuality v . Integrating over fractional virtuality defines the lightcone momentum distribution of a nucleon

$$\rho_N^A(\alpha) = \int_{-\infty}^0 dv \tilde{\rho}_N^A(\alpha, v), \tag{2}$$

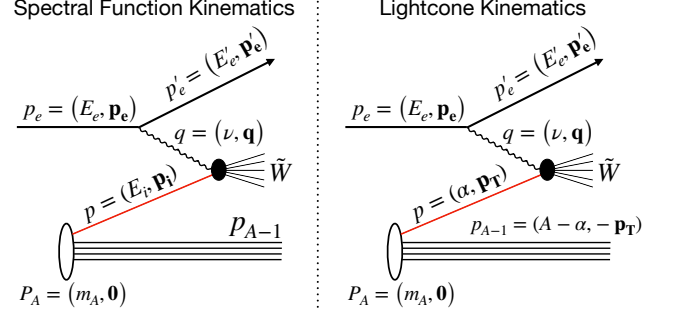


Fig. 1. Reaction diagram for lepton-nuclear deep inelastic scattering in a factorized plane wave impulse approximation. Red lines represent off-shell nucleons. See text for details.

that is normalized herein according to the baryon sum rule:

$$\int_0^A \frac{d\alpha}{\alpha} \rho_N^A(\alpha) \equiv 1. \tag{3}$$

To avoid producing an artificial EMC like effect in nucleon-only models when used in Eq. 1 [20], $\rho_N^A(\alpha)$ must also satisfy the momentum sum rule:

$$\frac{1}{A} \int_0^A \frac{d\alpha}{\alpha} \alpha \left(Z\rho_p^A(\alpha) + N\rho_n^A(\alpha) \right) = 1. \tag{4}$$

It is necessary to know the functional form of $\tilde{\rho}_N^A(\alpha, v)$ to proceed further. Although the nuclear wave functions for nuclei with $A = 2$ and $A = 3$ have been well-computed, they do not suffice to unambiguously yield the light-cone momentum distributions and their dependence on virtuality. This is because current calculations are non-relativistic and made with an underlying assumption that the nucleons are on their mass shell. Handling this issue on a fundamental level would require a first-principles light-front calculation including the effects of off-mass-shell dependence. Such a calculation could be done by solving the relevant Bethe-Salpeter equation, but does not yet exist.

Therefore, we consider here two approximations to estimate $\tilde{\rho}(\alpha, v)$: a spectral-function (SF) approximation, where the momentum sum rule is violated if only nucleonic degrees of freedom are taken into account, and a generalized-contact formalism lightcone (GCF-LC) approximation.

Spectral function approximation

The nuclear spectral function $S(E, p)$ defines the probability for finding a nucleon in the nucleus with momentum p and nucleon energy E . Exactly calculable spectral

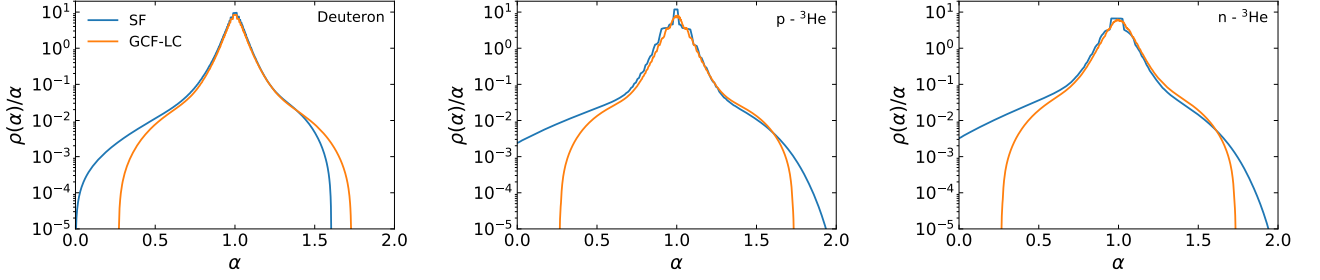


Fig. 2. Lightcone momentum distributions $\rho(\alpha)$ for deuteron (left) and protons (center) and neutrons (right) in ${}^3\text{He}$ calculated using the spectral function (SF) and generalized contact formalism lightcone (GCF-LC) approximations. The discretization visible in the SF distributions (blue lines) is due to the discretization of the spectral function $S(E, p)$ and integration of Eq. 5.

functions are available for light nuclei and allow calculating the nuclear lightcone distributions as [24, 25]

$$\tilde{\rho}_{N,SF}^A(\alpha, v) = \int dE d^3\mathbf{p} S_N^A(E, p) \cdot \frac{E + p_z}{E} \delta\left(\alpha - \frac{Ap^+}{P^+}\right) \delta\left(v - \frac{E^2 - |\mathbf{p}|^2 - m_N^2}{m_N^2}\right), \quad (5)$$

where $p = |\mathbf{p}|$, $p^+ \equiv E + p_z = m_A\alpha/A$ is the plus-component of the momentum of the struck nucleon, $P^+ = m_A$ is the plus-component of the momentum of the nucleus A , and m_A is the nucleus mass.

The flux factor $(E + p_z)$ is introduced to help satisfy the momentum sum rule [20]. The $\frac{1}{E}$ factor ensures SF-based lightcone distribution functions are appropriately normalized according to the Baryon sum-rule (Eq. 3). However, this also changes the interpretation of $\rho(\alpha)$ from a simple probability density for finding a nucleon in a nucleus with lightcone momentum fraction α (see discussion in refs. [20, 24, 25]).

For deuterium, considering a wave function calculated using the AV18 interaction, the momentum sum rule has a negligible violation ($< 0.1\%$). For ${}^3\text{He}$, using the AV18-based spectral function of Ref. [26], it is violated by $\leq 1\%$. This small violation is expected to produce an artificial EMC effect [20] that should result in a smaller nucleon modification effect required to explain the experimental data.

Generalized-contact formalism lightcone approximation

To fully satisfy the ${}^3\text{He}$ momentum sum rule, we examine an alternative approach for calculating $\tilde{\rho}_{N,SF}^A(\alpha, v)$ using a scale-separation approximation where the lightcone density function is separated into a mean-field (single-nucleon) part and an SRC part [14, 27–30]:

$$\tilde{\rho}_{N,GCF-LC}^A(\alpha, v) = \tilde{\rho}_{N,GCF,SRC}^A(\alpha, v) + \tilde{\rho}_{N,MF}^A(\alpha, v). \quad (6)$$

The SRC part of the lightcone density can be formulated by integrating over the lightcone SRC decay function [30, 31], which describes the distribution of the momentum of the struck nucleon as well as its partner, here denoted the ‘spectator’ nucleon:

$$\tilde{\rho}_{N,GCF,SRC}^A(\alpha, v) = \int d^2\mathbf{p}_\perp \frac{d\alpha_s}{\alpha_s} d^2\mathbf{p}_{s,\perp} \rho_{SRC}^N(\alpha, \mathbf{p}_\perp, \alpha_s, \mathbf{p}_{s,\perp}^\perp) \times \delta\left(v - \frac{p^-(m_A/A)\alpha - \mathbf{p}_\perp^2 - m_N^2}{m_N^2}\right), \quad (7)$$

where

$$p^- = P^- - p_s^- - p_{A-2}^- \\ = m_A - \frac{m_N^2 + (\mathbf{p}_s^\perp)^2}{(m_A/A)\alpha_s} - \frac{m_{A-2}^2 + (\mathbf{p}_{CM}^\perp)^2}{(m_A/A)(A - \alpha - \alpha_s)} \quad (8)$$

is the off-mass shell minus-component of the struck nucleon’s momentum, α_s is the spectator nucleon lightcone fraction, \mathbf{p}_\perp and $\mathbf{p}_{s,\perp}$ are the transverse momentum of the struck nucleon and the spectator, respectively, and $\mathbf{p}_{CM}^\perp = \mathbf{p}_\perp + \mathbf{p}_{s,\perp}$. ρ_{SRC}^N is a two-body (i.e. pair) lightcone density given by a convolution of the pair center-of-mass and relative momentum densities, see Ref. [30] and online supplementary materials for details.

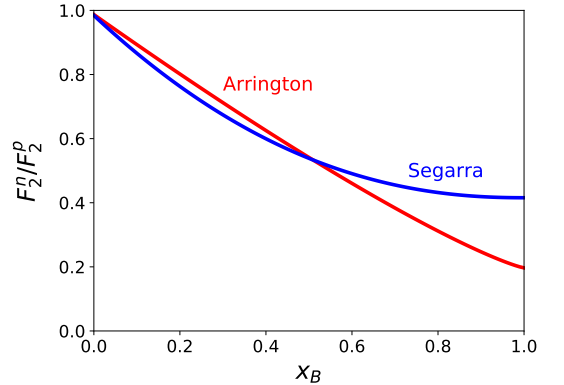


Fig. 3. F_2^n/F_2^p parametrizations used in this work that span the current range of models [15]. See text for details.

The mean-field part of the lightcone density is taken from the spectral functions using a linearized approximation, similar to Eq. 5, but which manifestly preserves the baryon number and momentum sum rules:

$$\begin{aligned} \tilde{\rho}_{N,MF}^A(\alpha, v) &= \alpha \int_0^{m_N} dE \int_0^{p_{cutoff}} d^3\mathbf{p} S_N^A(E, p) \\ &\times \delta\left(\alpha - 1 - \frac{Ap_z}{P^+}\right) \delta\left(v - \frac{E^2 - |\mathbf{p}|^2 - m_N^2}{m_N^2}\right). \end{aligned} \quad (9)$$

The cutoff momentum $p_{cutoff} = 240$ MeV/ c for ${}^3\text{He}$ and was chosen such that the fraction of SRC pairs was equal to that extracted from ab-initio many-body calculations (10.1% for neutrons and 5.9% for protons) [32, 33].

We emphasize that the momentum sum rule for $\tilde{\rho}_{N,GCF-LC}^A(\alpha, v)$ is manifestly satisfied in this approximation and that the resulting GCF-LC density is symmetric around unity, in contrast to that obtained in the SF approximation (Fig. 2).

STRUCTURE FUNCTION AND MODIFICATION MODELS

We compute Eq. 1 using parameterizations of $f^{off}(\tilde{x})$, $F_2^p(\tilde{x})$, and $\frac{F_2^n(\tilde{x})}{F_2^p(\tilde{x})}$, and both $\tilde{\rho}_{N,SF}^A$ and $\tilde{\rho}_{N,GCF-LC}^A$. For the modification function $f^{off}(\tilde{x})$ we consider three models:

$$f_{const}^{off}(\tilde{x}) = C, \quad (10)$$

$$f_{lin\ x}^{off}(\tilde{x}) = a + b \cdot \tilde{x} \quad (11)$$

$$f_{KP,CJ}^{off}(\tilde{x}) = C(x_0 - \tilde{x})(x_1 - \tilde{x})(1 + x_0 - \tilde{x}) \quad (12)$$

where f_{const}^{off} assumes a virtuality-dependent modification model that is independent of \tilde{x} , and $f_{lin\ x}^{off}$ is also linearly dependent on \tilde{x} . The free parameters of these parameterizations (C , a , and b) are determined by fitting Eq. 1 to experimental data as detailed below.

We also use modification functions determined by KP (f_{KP}^{off}) [34] and CJ (f_{CJ}^{off}) [35], who both chose to use a 3rd order polynomial in \tilde{x} , albeit with different parameters. These are used here with their original parameters, extracted in Refs. [34, 35].

$\frac{F_2^n(\tilde{x})}{F_2^p(\tilde{x})}$ was parametrized as:

$$\frac{F_2^n(\tilde{x})}{F_2^p(\tilde{x})} \equiv R_{np}(\tilde{x}) = a_{np} (1 - \tilde{x})^{b_{np}} + c_{np}, \quad (13)$$

where $R_{np}(\tilde{x} \rightarrow 1) = c_{np}$. We fix the a_{np} , b_{np} , and c_{np} parameters by fitting Eq. 13 to one of two recent predictions by Segarra [15] and by Arrington [36], that represent two extreme models that capture the spread of current models [15] (see Fig. 3). We further assume that $R_{np}(\tilde{x})$ has negligible Q^2 dependence. We note that the original f_{KP}^{off} and f_{CJ}^{off} extractions were done using

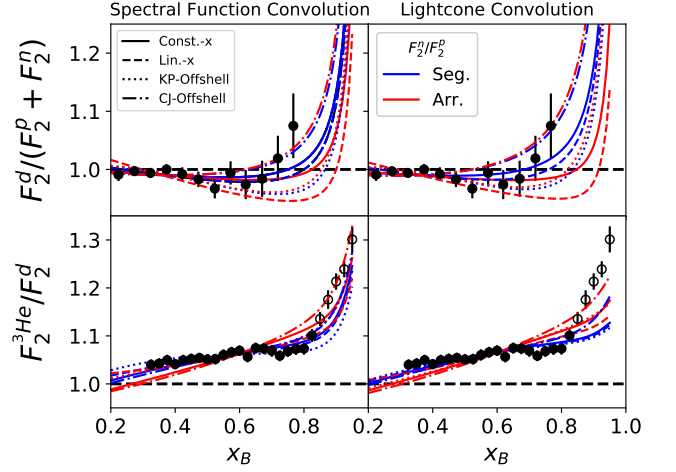


Fig. 4. Convolution results after χ^2 -minimization procedure. Each model is shown with the renormalization inferred for ${}^2\text{H}$ and ${}^3\text{He}$ and the resulting χ^2 . Open circles denote data at $W < 1.4$ GeV, which was not used in the fit. (Top-left) SF convolution results on $F_2^d / (F_2^p + F_2^n)$. (Top-right) LC convolution results on $F_2^d / (F_2^p + F_2^n)$. (Bottom-left) SF convolution results on $F_2^{3\text{He}} / F_2^d$. (Bottom-right) LC convolution results on $F_2^{3\text{He}} / F_2^d$. All curves are calculated and extrapolated with the same Q^2 as the data for ${}^2\text{H}$ and ${}^3\text{He}$.

F_2^n / F_2^p that are respectively similar to the Segarra and Arrington models used herein.

$F_2^p(x_B, Q^2)$ was taken from GD11-P [37]. As DIS data are typically given in the form of F_2^A / F_2^d ratios to minimize higher twist effects, the only explicit Q^2 dependence we assume is that of $F_2^p(x_B, Q^2)$, that is assumed to be negligible in the ratio F_2^n / F_2^p .

We estimated the parameters of f_{const}^{off} and $f_{lin\ x}^{off}$ using a χ^2 -minimization inference from a simultaneous fit to both $F_2^{3\text{He}} / F_2^d$ [6] and $F_2^d / (F_2^p + F_2^n)$ [38] data for $0.17 \leq x_B \leq 0.825$. While data for $F_2^{3\text{He}} / F_2^d$ of [6] extends up to $x_B \sim 0.9$, these high- x_B data are at low invariant mass, W . Requiring $W > 1.4$ GeV ($W^2 > 2$ GeV 2) in the fitting procedure limited the data to $x_B \leq 0.825$. However, we extrapolate our predictions up to $x_B \sim 0.95$ for use by future measurements, such as MARATHON [16]. Isoscalar corrections previously applied to $F_2^{3\text{He}} / F_2^d$ data were removed and the quoted experimental normalization uncertainties of each data set were accounted for in the fit. In the calculation of each data point, F_2^p is evaluated at the Q^2 value of the data. We performed 16 inference trials for different model assumptions for $\tilde{\rho}(\alpha, v)$, F_2^n / F_2^p and f^{off} (see Tab. I).

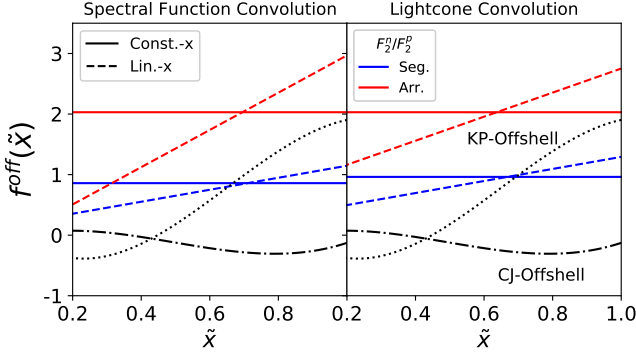


Fig. 5. Offshell functions $f^{off}(\tilde{x})$ resulting from χ^2 -minimization procedure with SF (left) and LC (right) approximations. The blue and red curves were minimization trials using a F_2^n/F_2^p fit to two recent predictions by Segarra [15] (Seg.) and Arrington [36] (Arr.), respectively. The two black lines are the offshell functions as described in [34, 35] and were taken as fixed for the minimization procedure which is why they are identical for both convolution frameworks.

RESULTS

Inclusive data description

Figure 4 shows the resulting fit compared to the experimental data. We performed eight individual fits, switching between the two F_2^n/F_2^p models, constant-in- \tilde{x} or linear-in- \tilde{x} offshell parameterizations, and using either SF or GCF-LC lightcone densities. We also show calculations using $f_{KP,CJ}^{off}$ and both F_2^n/F_2^p and lightcone densities. For completeness, Fig. 5 shows the inferred offshell functions for f_{const}^{off} and f_{lin-x}^{off} for the different convolution frameworks, along with $f_{KP,CJ}^{off}$ [34, 35].

As can be seen from the strong overlap of many curves, these existing ^3He and ^2H data cannot definitely discriminate between the different off-shell function or nucleon motion effect models. The data can be adequately reproduced even with very different off-shell models.

Tab. I and Fig. 4 do show a systematic improvement when using the Segarra et al. F_2^n/F_2^p parametrization (blue curves). Using f_{KP}^{off} , the calculation does not describe the high- x_B ^2H data. This is not unexpected as their offshell function was not fit to BONUS data nor to high- x_B deuterium data (≥ 0.8) [34]. f_{KP}^{off} does describe the ^3He EMC data markedly well due to the global nature of their analysis which captures the general EMC trend in a wide range of nuclei. Similarly, when using f_{CJ}^{off} , the calculation struggles as much as other models to accurately predict the ^3He EMC ratio. However, we note that their global fit does not consider $A > 2$ nuclear DIS data. Again, the agreement improves with the use of the Segarra et al. F_2^n/F_2^p .

The best fits with the Segarra et al. F_2^n/F_2^p (blue curves) and Arrington (red curves) find a comparable off-

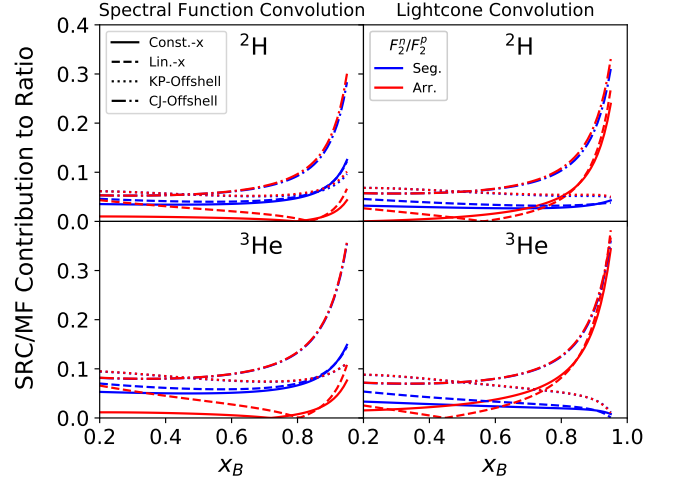


Fig. 6. Ratio of SRC contribution to MF contribution of the structure function. See text for details. (Top-left) SF ratio on F_2^d . (Top-right) LC ratio on F_2^d . (Bottom-left) SF ratio on $F_2^{^3\text{He}}$. (Bottom-right) LC ratio on $F_2^{^3\text{He}}$. Curves are shown with $Q^2 = 5 \text{ GeV}^2$

shell function f^{off} with the LC approximation as compared to the SF approximation, see Fig. 5.

The GCF-LC framework does just as well at describing the ^3He data and deuterium data, again, with improve-

TABLE I. Reduced χ^2 results of 16 trials with various model assumptions. $\tilde{\rho}(\alpha, \nu)$ refers to the approximation that was used for the lightcone virtuality and momentum distribution to calculate Eq. 1. Similarly, f^{off} refers to the offshell functional form used. There is a systematic increase in χ^2 when using F_2^n/F_2^p of Arrington [36]. There is also an increase when using GCF-LC approximation to $\tilde{\rho}(\alpha, \nu)$. We note that when using the KP and CJ off-shell parametrization there are no free parameters fit to data and the quoted χ^2 values show the quality of their description of the data without any minimization procedure.

$\tilde{\rho}(\alpha, \nu)$	F_2^n/F_2^p	$f^{off}(\tilde{x})$	χ_d^2	$\chi_{^3\text{He}}^2$	$\chi_{tot}^2/\text{d.o.f.}$
SF	Seg.	Const.-x	7.4	12.4	19.8 / 31 = 0.63
		Lin.-x	7.7	7.7	15.4 / 30 = 0.51
		KP	12.9	12.1	25 / 32 = 0.78
		CJ	6.6	23.4	30 / 32 = 0.94
	Arr.	Const.-x	17.4	69.1	86.5 / 31 = 2.79
		Lin.-x	25.9	16.0	41.9 / 30 = 1.40
		KP	12.1	21.4	33.5 / 32 = 1.05
		CJ	6.7	111.9	118.6 / 32 = 3.71
GCF-LC	Seg.	Const.-x	8.4	19.2	27.6 / 31 = 0.89
		Lin.-x	7.2	16.4	23.6 / 30 = 0.79
		KP	9.8	10.5	20.3 / 32 = 0.63
		CJ	11.8	26.8	38.6 / 32 = 1.21
	Arr.	Const.-x	22.9	69.3	92.2 / 31 = 2.97
		Lin.-x	25.4	53.1	78.5 / 30 = 2.62
		KP	8.7	64.5	73.2 / 32 = 2.29
		CJ	12.9	110.8	123.7 / 32 = 3.87

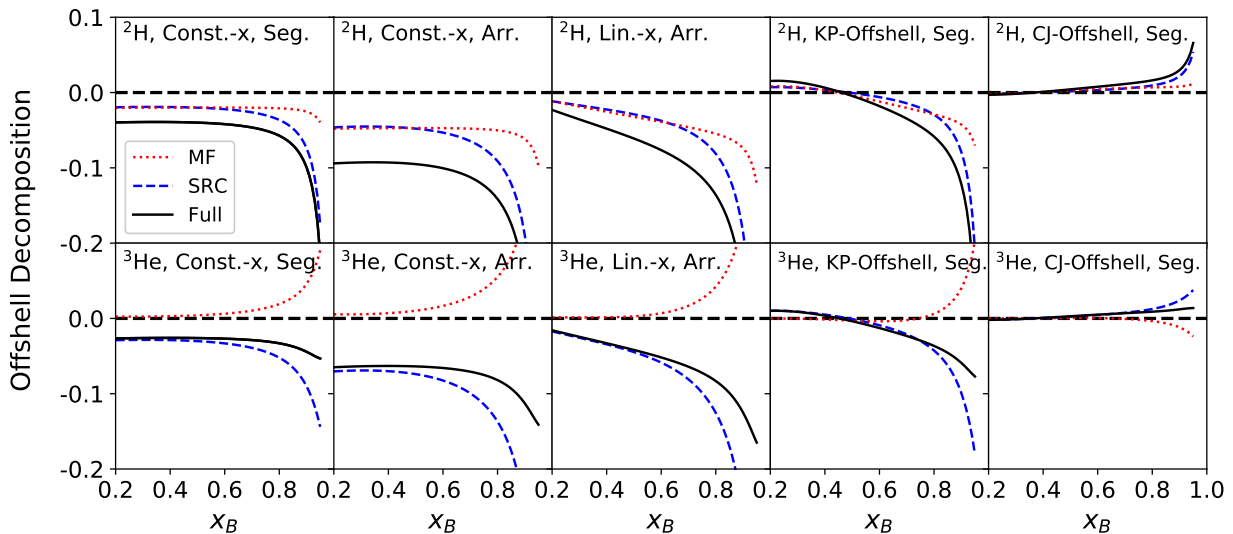


Fig. 7. Decomposition of $F_2^A(\text{offshell})$ for various model assumptions within the SF approximation. Top: offshell effect in ${}^2\text{H}$ for model assumptions of (from left-to right) 1) constant-in- x with Seg. F_2^n/F_2^p , 2) constant-in- x with Arr. F_2^n/F_2^p , 3) linear-in- x with Arr. F_2^n/F_2^p , 4) KP-offshell function with Seg. F_2^n/F_2^p , and 5) CJ-offshell function with Seg. F_2^n/F_2^p . Bottom: offshell effect in ${}^3\text{He}$ for the same models. Solid black lines represent the full offshell contribution. Dashed blue lines are the contribution due to SRC nucleons (> 240 MeV/c in the SF assumption). Similarly, dotted red lines are the contribution due to MF nucleons (< 240 MeV/c). Curves not shown for other model assumptions considered can be viewed in the online supplementary materials. Curves are shown at $Q^2 = 5$ GeV 2 .

ment with the use of the Segarra et al. F_2^n/F_2^p . In the GCF-LC framework, the high- x_B ${}^3\text{He}$ data not used in the fitting procedure (due to having low- W) is not as well described as in the SF framework. We also note that the f_{CJ}^{off} did not use ${}^3\text{He}$ data as a constraint, and, therefore, struggles at describing the data, especially at high- x_B .

SRC contribution to nucleon modification

Using the inferred parameters from the global fit as described above, we can now separate the contributions of the mean-field and SRC nucleons to the EMC effect. To this end we constructed $F_2^A = F_2^A(MF) + F_2^A(SRC)$ by splitting the integral in Eq. 1 to contributions of Mean-Field and SRC nucleons. This separation is natural for the GCF-LC approach. For the SF based approach this is done by assigning all nucleons with moment above 240 MeV/c as members of SRC pairs. Our findings are largely insensitive to the exact momenta we choose.

Figure 6 shows the ratio of the structure functions: $\left[F_2^{3He}(SRC) \right] / \left[F_2^{3He}(MF) \right]$ and $\left[F_2^d(MF) \right] / \left[F_2^d(SRC) \right]$. As expected, mean-field nucleons account for most of the structure function in Eq. 1, except at very high- x_B where nucleon motion effects are important and therefore the contribution of SRCs becomes significant. This is to be expected as SRC nucleons account for a small fraction of the nuclear

wave function, especially in deuterium.

Next we explicitly examine the contribution of mean-field and SRC nucleons to the offshell modification effect in the EMC. This is done by defining the offshell decomposition as $F_2^A(\text{offshell}) = F_2^A(\text{full}) - F_2^A(\text{no offshell})$, where $F_2^A(\text{full})$ is calculated using Eq. 1 and $F_2^A(\text{no offshell})$ is calculated using the same equation but by setting $f^{off}(\tilde{x}) = 0$.

Figure 7 shows the decomposition of $F_2^A(\text{offshell})$ due to SRC and mean-field nucleons within the SF approach (LC calculations are qualitatively similar and can be found in the online supplementary materials). While high momentum nucleons did not significantly contribute to the full convolution ratio in Fig. 6, these nucleons dominate the offshell modification function (i.e., the dashed blue lines track the solid black lines closely, especially at high x_B) in all models even though the offshell behavior is different for each model.

This holds true even in deuterium at high x_B , although at $x_B \sim 0.6$, the mean-field and SRC contributions are closer to 1:1. This is still surprising given the high-momenta fraction of the nuclear momentum-distribution is only $O(\sim 4\%)$ [39]. Adding to this surprise is the feature that a significant contribution to the wave function comes from np separations larger than the range of the nuclear forces [40].

Furthermore, in the results shown here using the SF approach, the momentum sum rule is violated by $\sim 1\%$. While small, this violation still induces an artificial EMC

effect, thereby reducing the strength of the actual offshell contribution to the structure function (i.e. the absolute y -scale of Fig. 7). Alternatively, in the LC approach, the sum rules are manifestly satisfied, and the extracted offshell contribution is much larger for the models of $F_2^n/F_2^p|_{Seg.}$ by a factor of about 1.5 – 3 (see online supplementary materials).

Our findings are robust to the exact underlying offshell function used in Eq. 1, even though $f^{off}(\tilde{x})$ (Fig. 5) varies dramatically among the models. Therefore, the results shown in Fig. 7 contradict the recent claims of Ref. [41], where the SRC UMF was analyzed without proper separating its contributions from nucleon motion and modification effects. For completeness we note that the UMF extracted by Ref. [7, 15] is reproduced with the convolution framework used here for ${}^3\text{He}$, see online supplementary materials.

PREDICTING FORTHCOMING OBSERVABLES

While existing data cannot constrain F_2^n/F_2^p , we predict F_2^{3H}/F_2^d , which was recently measured by the MARATHON collaboration [16], and should be sensitive to F_2^n . Fig. 8 shows the convolution prediction for F_2^{3H}/F_2^d obtained using the constrained offshell modification function and assuming isospin symmetry in the lightcone distributions. The different F_2^n/F_2^p parametrizations, which are both consistent with F_2^{3He}/F_2^d data, predict very different F_2^{3H}/F_2^d at high- x_B that MARATHON can test. Still, as seen in Fig. 8, there are predictions of F_2^{3H}/F_2^d which overlap for very different F_2^n/F_2^p and f^{off} behaviors. In particular, taking the f_{KP}^{off} with $F_2^n/F_2^p|_{Seg.}$ (blue dotted) and f_{CJ}^{off} with $F_2^n/F_2^p|_{Arr.}$ (red dash-dotted), yield overlapping predictions. This indicates a combined analysis of nuclear DIS data with forthcoming data by MARATHON will be needed to disentangle F_2^n/F_2^p and f^{off} , similar to efforts Ref. [34] has performed in the past.

While the MARATHON results will be very sensitive to F_2^n/F_2^p , they will be less sensitive to the exact nature of the offshell modification function (f^{off}). This can however be tested in a new set of tagged deep inelastic scattering measurements off deuterium which will study the dependence of the bound nucleon structure function on α :

$$F_2^{p*}(\tilde{x}, \alpha) = F_2^p(\tilde{x}) \left[1 + \langle v \rangle |_{\alpha} f^{off}(\tilde{x}) \right], \quad (14)$$

where $\langle v \rangle |_{\alpha}$ is the average fractional virtuality for the given α , see online supplementary materials Figs. 1 and 2.

By taking a ratio of the bound-to-free proton structure function, one can access the offshell modification function, and can examine the differences of the offshell contribution at high- \tilde{x} and low- \tilde{x} , see Fig 9. The predictions here are similar to those made by Ref. [42] and will

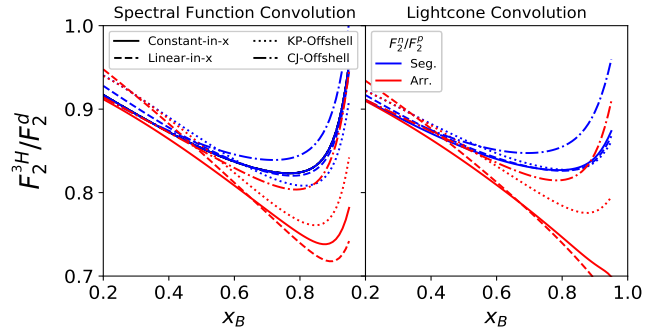


Fig. 8. Predictions of $\frac{F_2^{3H}}{F_2^d}$ using our convolution framework with the universal offshell modification constrained from ${}^2\text{H}$ and ${}^3\text{He}$ data: (Left) SF convolution, (Right) LC convolution. See text for details. All curves are shown for MARATHON kinematics, i.e., $Q^2 = 14 \cdot x_B$ [GeV 2].

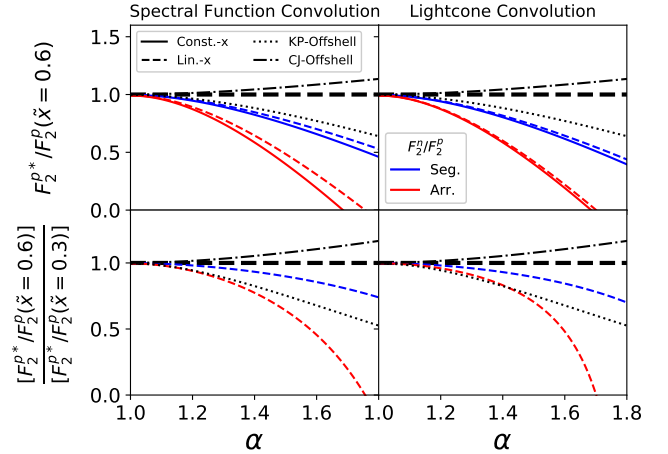


Fig. 9. Predictions of the ratio of the bound proton structure function in deuterium to the free proton structure function as a function of α . In the bottom panels, predictions for models with f_{const}^{off} yield a double ratio of 1, as the modification is constant in \tilde{x} . See text for details. Curves are shown at $Q^2 = 5$ GeV 2 and for $\mathbf{p}_T = 0$.

be directly tested by the LAD [18] and BAND [17] Collaborations. The latter already completed 50% data taking and results are anticipated soon. While predictions here are made for $\mathbf{p}_T = 0$, experiments will have some finite acceptance in \mathbf{p}_T . As seen in Fig 9, there are significant uncertainties due to uncertainties in F_2^n/F_2^p (red vs. blue curves). However, after precise measurements on F_2^n/F_2^p by the MARATHON Collaboration [16], these uncertainties will be greatly reduced.

SUMMARY

We present an extensive study of nucleon modification effects in nuclei using a convolution formalism and measurements of the EMC effect in deuterium and ^3He . We examine a range of off-shell modification functions, free-neutron structure function models and different treatments of nucleon motion effects. In all cases we find that nucleons in SRC pairs are the dominant contribution to nucleon modification effects in deuterium and ^3He .

With upcoming precise measurements of ^3H , our study can be extended to test the isospin dependence of the universal offshell modification function and the ability to use nuclear DIS data to constrain the free neutron structure function. We stress that an isospin-dependent EMC effect, in the sense of a different average modification for protons and neutrons, as e.g. suggested by Refs. [10, 43, 44], can be obtained in all models discussed in this paper if the proton and neutron lightcone densities have different average virtualities. In addition we make predictions for new measurements of the bound nucleon structure function. These measurements will allow us to further constrain the elements of our model.

This work was supported by the U.S. Department of Energy, Office of Science, Office of Nuclear Physics under Award Numbers DE-FG02-94ER40818, DE-FG02-96ER-40960, DE-AC05-06OR23177, DE-FG02-93ER-40771, and DE-FG02-97ER-41014 under which Jefferson Science Associates operates the Thomas Jefferson National Accelerator Facility, the Pazy foundation, and the Israeli Science Foundation (Israel) under Grants Nos. 136/12 and 1334/16.

* Contact Author hen@mit.edu

- [1] R. G. Arnold, P. E. Bosted, C. C. Chang, J. Gomez, A. T. Katramatou, G. G. Petratos, A. A. Rahbar, S. E. Rock, A. F. Sill, Z. M. Szalata, A. Bodek, N. Giokaris, D. J. Sherden, B. A. Mecking, and R. M. Lombard, “Measurements of the a dependence of deep-inelastic electron scattering from nuclei,” *Phys. Rev. Lett.* **52**, 727–730 (1984).
- [2] J.J. Aubert *et al.*, *Phys. Lett. B* **123**, 275 (1983).
- [3] J. Ashman *et al.*, “Measurement of the ratios of deep inelastic muon-nucleus cross sections on various nuclei compared to deuterium,” *Phys. Lett. B* **202**, 603 (1988).
- [4] J. Gomez *et al.*, “Measurement of the a dependence of deep-inelastic electron scattering,” *Phys. Rev. D* **49**, 4348 (1994).
- [5] M. Arneodo *et al.*, “Measurements of the nucleon structure function in the range $0.002 < x < 0.17$ and $0.2 < q^2 < 8 \text{ geV}^2$ in deuterium, carbon and calcium,” *Nucl. Phys. B* **333**, 1 (1990).
- [6] J. Seely *et al.*, “New measurements of the european muon collaboration effect in very light nuclei,” *Phys. Rev. Lett.* **103**, 202301 (2009).
- [7] B. Schmookler *et al.* (CLAS Collaboration), “Modified structure of protons and neutrons in correlated pairs,” *Nature* **566**, 354–358 (2019).
- [8] Leonid Frankfurt and Mark Strikman, “Hard nuclear processes and microscopic nuclear structure,” *Phys. Rep.* **160**, 235 – 427 (1988).
- [9] P R Norton, “The EMC effect,” *Reports on Progress in Physics* **66**, 1253–1297 (2003).
- [10] O. Hen, G. A. Miller, E. Piasetzky, and L. B. Weinstein, “Nucleon-Nucleon Correlations, Short-lived Excitations, and the Quarks Within,” *Rev. Mod. Phys.* **89**, 045002 (2017).
- [11] D. M. Alde *et al.*, “Nuclear dependence of dimuon production at 800-GeV. FNAL-772 experiment,” *Phys. Rev. Lett.* **64**, 2479–2482 (1990).
- [12] L. B. Weinstein, E. Piasetzky, D. W. Higinbotham, J. Gomez, O. Hen, and R. Shneor, “Short range correlations and the emc effect,” *Phys. Rev. Lett.* **106**, 052301 (2011).
- [13] O. Hen, E. Piasetzky, and L. B. Weinstein, “New data strengthen the connection between short range correlations and the emc effect,” *Phys. Rev. C* **85**, 047301 (2012).
- [14] Or Hen, D. W. Higinbotham, Gerald A. Miller, Eli Piasetzky, and Lawrence B. Weinstein, “The EMC Effect and High Momentum Nucleons in Nuclei,” *Int. J. Mod. Phys. E22*, 1330017 (2013), [arXiv:1304.2813 \[nucl-th\]](https://arxiv.org/abs/1304.2813).
- [15] E. P. Segarra, A. Schmidt, D. W. Higinbotham, E. Piasetzky, M. Strikman, L. B. Weinstein, and O. Hen, “Flavor dependence of the nucleon valence structure from nuclear deep inelastic scattering data,” *Phys. Rev. Lett.* (2020), [arXiv:1908.02223 \[nucl-th\]](https://arxiv.org/abs/1908.02223).
- [16] G. G. Petratos *et al.*, “Measurement of the F_2^n/F_2^p , d/u Ratios and $A = 3$ EMC Effect in Deep Inelastic Electron Scattering Off the Tritium and Helium Mirror Nuclei,” Jefferson Lab PAC36 Proposal (2010).
- [17] O. Hen *et al.*, “In medium proton structure functions, src, and the emc effect,” JLab PAC Proposal (2015).
- [18] O. Hen, L.B. Weinstein, S.A. Wood, and S. Gilad, “In Medium Nucleon Structure Functions, SRC, and the EMC effect, Jefferson Lab experiment E12-11-107,” (2011).
- [19] L. L. Frankfurt and M. I. Strikman, “Point-like Configurations in Hadrons and Nuclei and Deep Inelastic Reactions with Leptons: EMC and EMC Like Effects,” *Nucl. Phys. B250*, 143–176 (1985).
- [20] L.L. Frankfurt and M.I. Strikman, “On the normalization of nucleus spectral function and the EMC effect,” *Phys. Lett. B183*, 254 (1987).
- [21] S.V. Akulinichev, S. Shlomo, S.A. Kulagin, and G.M. Vagradov, “Lepton-Nucleus Deep-Inelastic Scattering,” *Phys. Rev. Lett.* **55**, 2239 (1985).
- [22] G.V. Dunne and A.W. Thomas, “The Effect of Conventional Nuclear Binding on Nuclear Structure Functions,” *Nucl.Phys. A455*, 701–719 (1985).
- [23] Gerald A. Miller, “Confinement in Nuclei and the Expanding Proton,” *Phys. Rev. Lett.* **123**, 232003 (2019), [arXiv:1907.00110 \[nucl-th\]](https://arxiv.org/abs/1907.00110).
- [24] H. Jung and Gerald A. Miller, “Pionic contributions to deep inelastic nuclear structure functions,” *Phys. Rev. C41*, 659 (1990).
- [25] H. Jung and Gerald A. Miller, “Nucleonic contribution to lepton-nucleus deep inelastic scattering,” *Phys. Lett. B200*, 351 (1988).
- [26] C. Ciofi degli Atti and L.P. Kaptari, “Calculations of the Exclusive Processes $2\text{H}(e,e'p)n$, $3\text{He}(e,e'p)2\text{H}$ and

- $^3\text{He}(e,e'p)(pn)$ within a Generalized Glauber Approach,” *Phys. Rev.* **C71** (2005), [10.1103/PhysRevC.71.024005](https://arxiv.org/abs/10.1103/PhysRevC.71.024005).
- [27] Claudio Ciofi degli Atti and S. Simula, “Realistic model of the nucleon spectral function in few and many nucleon systems,” *Phys. Rev. C* **53**, 1689 (1996).
- [28] C. Ciofi degli Atti, L.L. Frankfurt, L.P. Kaptari and M.I. Strikman, “On the dependence of the wave function of a bound nucleon on its momentum and the emc effect,” *Phys. Rev. C* **76**, 055206 (2007).
- [29] Ronen Weiss, Igor Korover, Eliezer Piasetzky, Or Hen, and Nir Barnea, “Energy and momentum dependence of nuclear short-range correlations - Spectral function, exclusive scattering experiments and the contact formalism,” *Phys. Lett.* **B791**, 242–248 (2019), [arXiv:1806.10217 \[nucl-th\]](https://arxiv.org/abs/1806.10217).
- [30] J. R. Pybus, I. Korover, R. Weiss, A. Schmidt, N. Barnea, D. W. Higinbotham, E. Piasetzky, M. Strikman, L. B. Weinstein, and O. Hen, “Generalized Contact Formalism Analysis of the $^4\text{He}(e, e'pN)$ Reaction,” (2020), [arXiv:2003.02318 \[nucl-th\]](https://arxiv.org/abs/2003.02318).
- [31] A. Schmidt *et al.* (CLAS), “Probing the core of the strong nuclear interaction,” *Nature* **578**, 540–544 (2020), [arXiv:2004.11221 \[nucl-ex\]](https://arxiv.org/abs/2004.11221).
- [32] R. Weiss, R. Cruz-Torres, N. Barnea, E. Piasetzky, and O. Hen, “The nuclear contacts and short range correlations in nuclei,” *Phys. Lett. B* **780**, 211 (2018).
- [33] R. Cruz-Torres, D. Lonardonì, R. Weiss, N. Barnea, D. W. Higinbotham, E. Piasetzky, A. Schmidt, L. B. Weinstein, R. B. Wiringa, and O. Hen, “Scale and Scheme Independence and Position-Momentum Equivalence of Nuclear Short-Range Correlations,” *arXiv* (2019), [arXiv:1907.03658 \[nucl-th\]](https://arxiv.org/abs/1907.03658).
- [34] S.A. Kulagin and R. Petti, “Global study of nuclear structure functions,” *Nuclear Physics A* **765**, 126 – 187 (2006).
- [35] A. Accardi, L. T. Brady, W. Melnitchouk, J. F. Owens, and N. Sato, “Constraints on large- x parton distributions from new weak boson production and deep-inelastic scattering data,” *Phys. Rev.* **D93**, 114017 (2016), [arXiv:1602.03154 \[hep-ph\]](https://arxiv.org/abs/1602.03154).
- [36] J. Arrington, J. G. Rubin, and W. Melnitchouk, “How Well Do We Know The Neutron Structure Function?” *Phys. Rev. Lett.* **108**, 252001 (2012), [arXiv:1110.3362 \[hep-ph\]](https://arxiv.org/abs/1110.3362).
- [37] A. Airapetian, N. Akopov, and Z. et al. Akopov, “Inclusive measurements of inelastic electron and positron scattering from unpolarized hydrogen and deuterium targets,” *J. High Energ. Phys.* **126** (2011), [10.1007/JHEP05\(2011\)126](https://arxiv.org/abs/10.1007/JHEP05(2011)126).
- [38] K. A. Griffioen *et al.*, “Measurement of the EMC Effect in the Deuteron,” *Phys. Rev.* **C92**, 015211 (2015), [arXiv:1506.00871 \[hep-ph\]](https://arxiv.org/abs/1506.00871).
- [39] S. Veerasamy and W. N. Polyzou, “Momentum-space argonne v18 interaction,” *Phys. Rev. C* **84**, 034003 (2011).
- [40] L. L. Frankfurt and M. I. Strikman, “On the problem of extracting the neutron structure function from ed scattering,” *Phys. Lett* **B76**, 333–336 (1978).
- [41] X.G. Wang, A.W. Thomas, and W. Melnitchouk, “Do short-range correlations cause the nuclear EMC effect in the deuteron?” (2020), [arXiv:2004.03789 \[hep-ph\]](https://arxiv.org/abs/2004.03789).
- [42] W. Melnitchouk, M. Sargsian, and M. Strikman, “Probing the origin of the EMC effect via tagged structure functions of the deuteron,” *Z. Phys.* **A359**, 99–109 (1997).
- [43] O. Hen *et al.*, “Momentum sharing in imbalanced Fermi systems,” *Science* **346**, 614–617 (2014), [arXiv:1412.0138 \[nucl-ex\]](https://arxiv.org/abs/1412.0138).
- [44] M. Duer *et al.* (CLAS Collaboration), “Probing high-momentum protons and neutrons in neutron-rich nuclei,” *Nature* **560**, 617–621 (2018).